

Simple Network Mechanism Leads to Quasi-Real Brain Activation Patterns with *Drosophila* Connectome

Xiaoyu Zhang¹, Pengcheng Yang¹, Jiawei Feng¹, Qiang Luo², Wei Lin², and Xin Lu^{*1}

¹College of Systems Engineering, National University of Defense Technology

²Institute of Science and Technology for Brain-Inspired Intelligence, Fudan University

Abstract

Considering the high computational demands of most methods, using network communication models to simulate the brain is a more economical way. However, despite numerous brain network communication models, there is still insufficient evidence that they can effectively replicate the real activation patterns of the brain. Moreover, it remains unclear whether actual network structures are crucial in simulating intelligence. Addressing these issues, we propose a large scale network communication model based on simple rules and design criteria to assess the differences between network models and real situations. We conduct research on the biggest adult *Drosophila* connectome data set. Experimental results show significant activation in neurons that should respond to stimulus and slight activation in irrelevant ones, which we call quasi-real activation pattern. Besides, when we change the network structure, the quasi-activation patterns disappear. Interestingly, activation regions have shorter network distances to their input neurons, implying that the network structure (not spatial distance) is the core to form brain functionality. In addition, giving the input neurons a unilateral stimulus, we observe a bilateral response, which is consistent with reality. Then we find that both hemispheres have extremely similar statistical indicators. We also develop real-time 3D large spatial network visualization software to observe and document experimental phenomena, filling the software gap. This research reveals network models power: it can reach the quasi-activation pattern even with simple propagation rules. Besides, it provides evidence that network structure matters in brain activity pattern generation. Future research could fully simulate brain behavior through network models, paving the way for artificial intelligence by developing new propagation rules and optimizing link weights.

Keywords: brain network, network communication model, *drosophila* connectome, activation pattern

1 Introduction

The neural systems of intelligent beings maintain constant communication [1] [2]. The intricate mechanism of this communication unfolds as follows: specific neurons, often input neurons, receive stimulus signals from the external environment or other parts of the body, transitioning from a resting to an activated state. Subsequently, they relay these stimulus signals to the next tier of neurons through synapses. This process gives rise to macroscopic emergence across the entire neural system. Such communication fosters the emergence of intelligence in all intelligent life forms, including humans. Consequently, comprehending and replicating this process has become an indispensable avenue for unraveling biological intelligence and realizing artificial intelligence [3].

Neural systems are interconnected networks [4], with neurons engaging in constant communication via synapses within the network's topology. The brain's unique and complex network structure is pivotal to the emergence of intelligence [5]. Many scientists posit that network science is crucial for deciphering the mechanisms underlying the flexible regulation of neural communication [6] [7] [8]. Determining how to leverage network science methodologies stands as a paramount challenge in contemporary neuroscience. Within this discipline, neural networks are often represented as graphs, consisting of nodes (entities) and edges (relationships). From the broadcasting model [9] to the diffusion model [10], researchers strive to craft network models that mimic activation patterns observed in the brain, offering insights into the workings of neural networks.

However, despite artificial neural networks (ANNs)' deviation from the brain's actual structure, they get full achievements in achieving intelligence, which cast doubt on the necessity of real network structures in brain behavior simulation. Furthermore, some researchers have highlighted the absence of evidence linking network model simulations to genuine brain activity patterns [11], undermining the models' status as a robust research tool in neuroscience. The effectiveness of network models in replicating the neuronal system's activation dynamics remains uncertain. This uncertainty partly stems from many models' failure to replicate the brain's structure at the neuron and synapse level, compromising the models' interpretability.

*Corresponding author: xin.lu.lab@outlook.com

Moreover, current brain network communication models often rely on prevalent metrics such as signaling cost and activation time to assess model quality [11]. Yet, these metrics fall short of verifying whether a network model accurately reflects the brain’s actual activation patterns, which is the fundamental goal of brain simulation. There is a need for evaluation criteria that can affirm whether network communication models genuinely mirror the brain’s communication processes. Additionally, observing the brain network communication process is important for researches. The absence of 3D visualization software capable of real-time monitoring of communication status and displaying networks with a vast number of nodes poses challenges for researchers, including neuroscientists, by impeding real-time observation, display, and analysis of experimental outcomes.

Over the past few decades, biologists have dedicated themselves to determining the precise structure of the connectome, ranging from *C. elegans* [12] to *Drosophila* larvae [13]. By understanding the connections within an organism’s nervous system, researchers can gain insights into how the nervous system operates. A recent study [14] has published the largest adult *Drosophila* connectome, providing data support for researches in network science.

For these reasons, we conducted experiments utilizing the recently released comprehensive data set of the largest adult *Drosophila* connectome, enhancing the interpretability of our findings. Our approach involves crafting a large scale network communication model based on simple mechanisms, designed to simulate the activation behavior observed in the connectome.

Specifically, We establish the network representation of the connectome. Then we design each neuron’s state and threshold functions. When a neuron’s state meets the threshold, it activates and subsequently transmits signals to other neurons. After a few iteration, the whole network emerges an activation pattern. Additionally, we propose an evaluation criteria based on the ratio of actually activated neurons to the expected number of activation. Experiments reveals that our model has significant activation in the type of neurons that should be affected by the stimulus and slight activation in irrelevant neurons which called a quasi-real activation pattern. To prove the vitalness of network structure, we calculate every node’s layer and shuffle part of the network structure in same layer and find the shuffled network can’t generate any quasi-real activation pattern.

To enhance our understanding, we developed a 3D network visualization software, utilizing HTML5’s Canvas and Three.js based on WebGL technology for large spatial network visualization effects. This tool enables real-time observation of each neuron’s communication process.

To prove the network structure matters (rather than spatial structure) in activation pattern generation, we calculate the average network and spatial distance of input and activation neurons and results reveal that the average network distance between input neurons and their corresponding activation areas is shorter than unrelated areas, which is a strong evidence to prove network structure matters in the process of message transmission in brain.

Furthermore, by subjecting input neurons to the same stimulus, we observe significant responses in neurons expected to be affected, with only slight responses in irrelevant neurons—characterized as a quasi-real activation pattern. Notably, when providing unilateral stimuli to input neurons, we observe a bilateral response in the *Drosophila* neuronal wiring diagram, aligning with reality. Then we calculate the statistics properties and find that the left and right hemispheres have extremely similar degree, clustering coefficient, and eigenvector centrality vector coefficient. The vectors’ Person coefficient are up to 0.9986, 0.9988, and 0.9991, respectively.

2 Related Works

Various models have been developed to mimic or understand aspects of brain function, ranging from the cellular level to the whole brain. In this section we review the models that aim to simulate the brain’s behavior. The review includes neural dynamic model that describes how action potentials in neurons are initiated and propagated. In addition, we introduce the large scale brain simulating methods. At last, we introduce the network communication models which refers to a computational or theoretical framework designed to understand and simulate how different parts of the brain communicate with each other.

2.1 Neuron Dynamic Model

In past years, neuroscientists have aimed to describing the behavior of neurons by dynamic model. One of the most famous works is the Hodgkin-Huxley (HH) model [15]. It includes a set of differential equations that describe the changes in membrane potential and the dynamics of ion channels. The key variables in the model are the membrane potential V , and the gating variables m , n , h that represent the probability of ion channels being open.

The currents are given by:

$$I_{Na} = \bar{g}_{Na} m^3 h (V - E_{Na}) \quad (1)$$

$$I_K = \bar{g}_K n^4 (V - E_K) \quad (2)$$

$$I_L = \bar{g}_L (V - E_L) \quad (3)$$

Where \bar{g}_{Na} , \bar{g}_K and \bar{g}_L are the maximum conductances for sodium, potassium, and leak channels. E_{Na} , E_K , and E_L are the reversal potentials for sodium, potassium, and leak channels.

The gating variables obey first-order kinetics and are described by the following differential equations:

$$\frac{dm}{dt} = \alpha_m(1 - m) - \beta_m m \quad (4)$$

$$\frac{dn}{dt} = \alpha_n(1 - n) - \beta_n n \quad (5)$$

$$\frac{dh}{dt} = \alpha_h(1 - h) - \beta_h h \quad (6)$$

Where m , n , and h are the gating variables representing the activation and inactivation states of the ion channels. α_m , α_n , α_h , β_m , β_n , and β_h are voltage-dependent rate constants for the gating variables. These rate constants are defined by empirical equations based on experimental data. HH model accurately describes the electrophysiological processes of neuronal activity through mathematical equations, allowing scientists to understand the fundamental mechanisms of a group of neurons' behavior at the molecular and cellular levels.

Another famous theory is cable theory [16]. Cable theory is a mathematical model used to understand how electrical signals propagate along neurons, especially in their dendrites and axons. This theory applies the principles of electrical circuits to describe how the passive properties of the neuron influence signal transmission. It's particularly useful in explaining the conduction of graded potentials, such as synaptic potentials and electrotonic (passive) spread of membrane potential changes.

The core equation of cable theory is derived from the cable equation, which is a form of the second-order linear partial differential equation. It can be expressed as:

$$\frac{\partial^2 V}{\partial x^2} = \frac{1}{r_m} \left(\frac{\partial V}{\partial t} + \frac{V}{r_c} \right) \quad (7)$$

, where V is the membrane potential, x is the distance along the cable, t is time, r_m is the membrane resistance per unit length, r_c is the cytoplasmic (axial) resistance per unit length. This equation describes how the voltage V changes along the length of the neuron x and over time t .

Cable theory has several important applications in neuroscience, including understanding signal decay, neural modeling and synaptic integration. Despite its usefulness, cable theory has limitations. First, real neurons have complex geometries, which are simplified in cable theory. This can lead to inaccuracies in predicting real neuronal behavior. The complex structure of neuron should not be neglected. Besides, cable theory primarily addresses passive electrical properties and does not account for active properties like action potentials, which are crucial for neural communication.

Apart from that, researchers proposed many variants of neuron dynamic models [17] [18]. These models serve to elucidate the physiological activity of neurons and contribute to the description of neuron behavior.

However, these models has some limitations: these equations often contain a multitude of parameters. In instances where measurement techniques fall short of quantifying each parameter individually, estimation becomes a necessity.

Spiking Neural Networks (SNNs) [19] is designed to optimize the parameters in neural dynamic models. Unlike their traditional counterparts, which process information through continuous values, SNNs utilize discrete events known as spikes. These spikes, brief in duration, mimic the communication method of neurons within the brain, facilitating the transmission of information.

One of the simplest and most commonly used models to describe neuron dynamics in SNNs [19] is the Leaky Integrate-and-Fire (LIF) model [20]. The LIF model captures the essential characteristics of spike generation in neurons. The membrane potential $V(t)$ of a neuron at time t is described by the following differential equation.

$$\tau_m \frac{dV(t)}{dt} = -[V(t) - V_{rest}] + RI(t) \quad (8)$$

Where τ_m is the membrane time constant, which determines how fast the membrane potential decays towards the resting potential V_{rest} in the absence of input. V_{rest} is the resting membrane potential. R is the membrane resistance. $I(t)$ is the input current at time t . When $V(t)$ reaches a certain threshold $V_{threshold}$, the neuron fires a spike, and $V(t)$ is reset to V_{rest} or another predefined value. After firing, the neuron may enter a refractory period during which it cannot spike, regardless of the input.

SNNs have enabled researchers to simulate networks comprising millions of neurons, tackling a wide array of tasks ranging from image classification and natural language processing to controlling robotic arms [21] [22] [23] [24].

Despite their advances, SNNs face significant challenges. One primary issue is that the SNN’s structure often draws inspiration from anatomically defined functional brain networks rather than accurately replicating the intricate neural connections observed at the microscale. In terms of the connection method of artificial neurons, SNNs usually use a structure similar to that of ANNs. Consequently, these models resort to architectures akin to those found in artificial neural networks, hindering their ability to authentically emulate brain functions. Additionally, SNNs are marked by their low computational efficiency, with a single forward propagation frequently requiring several seconds to complete. These limitations underscore the difficulties in considering SNNs as the optimal approach for brain simulation in their current state.

As for the large scale brain simulation model aims to simulate the whole brain’s behavior, Eugene et al. [25] present the first large-scale brain simulation model based on experimental measures in several mammalian species. The model is founded upon the global thalamocortical anatomy derived from diffusion tensor imaging of the human brain. It incorporates multiple thalamic nuclei and a six-layered cortical microcircuitry, which is grounded in in vitro labeling and three-dimensional reconstruction of single neurons from the cat visual cortex. Additionally, the model simulates over 1,000,000 SNN neurons, calibrated to replicate known in vitro response patterns recorded in rats. It boasts nearly half a billion synapses, incorporating accurate receptor kinetics, short-term plasticity, and dendritic spike-timing-dependent synaptic plasticity (dendritic STDP). The model can demonstrate behavioral patterns that mimic normal brain activity. This model is a comprehensive attempt to simulate the whole neural system, which is a critical component of the brain involved in sensory processing and consciousness.

Eliasmith et al. [26] introduce a more comprehensive brain simulating model, which consists of 2,500,000 neurons and serves to close this divide by demonstrating a variety of behaviors. This model receives only sequences of visual images and produces all its responses through a simulated arm. Despite its simplifications of real structure, the model encapsulates numerous elements of neuroanatomy, neurophysiology, and behavioral psychology, as evidenced by its performance across eight distinct tasks.

As for the standardized platform, Zeng et al. [27] present BrainCog, a cognitive intelligence engine inspired by the brain. This platform, based on SNN, offers critical infrastructure for the creation of brain-inspired artificial intelligence and simulation of the brain. BrainCog encompasses a variety of biological neurons, encoding methods, learning principles, brain regions, and a combination of hardware and software as its core elements.

However, it is essential to note that each neuron’s dynamic model involves multiple differential equations, posing a significant challenge in simulating the complete behavior of the intact brain given the constraints of available computing power. Therefore, there is a compelling need for a cost-effective simulation approach to address this challenge.

As for the collective action of neuron populations, despite the success of neural system mean field models [28] in areas such as modeling epileptic seizures [29], there is still a lack of models that precisely describe the large-scale activity of whole brain.

2.2 Brain Network Communication Model

The network communication model is a conceptual framework that describes how data is transmitted from one node to another over a network. It breaks down the complex process of communication into simpler, more manageable layers or components, each with a specific role. The most widely recognized network communication models are the Open Systems Interconnection (OSI) model and the Internet Protocol Suite, commonly known as the TCP/IP model. Nowadays, scientists apply network communication models to neuron research, which are mostly used to understand how brain networks operate [30] [31] [32].

Early studies have indicated that, similar to social and electrical networks [33], brain networks also exhibit properties such as power-law distributions [34] and the rich-club phenomenon [35]. These results indicate that brain networks contain a wealth of network statistical characteristics. To reveal the mystery of the brain, researchers must take network characteristics into consideration.

Researchers designed many brain network models to describe the processes of message propagation in brain. One category of brain network communication models is the routing protocol model. The most famous model of this category is shortest path model [36], which assumes that signals between a pair of nodes travel along the shortest path between them. Let $d(v)$ represent the shortest path length from the starting node to node v , for each node v in the network, initialize $d(v) = \infty$, then for the starting node s , set $d(s) = 0$. Next, process each node in increasing order of $d(v)$, for each node, update the $d(u)$ value of its neighbors u . The update way can be represented as follows:

$$d(u) = \min(d(u), d(v) + w(v, u)) \quad (9)$$

where $w(v, u)$ is the weight of edge e_{uv} .

However, the key disadvantage of the model is these methods require each neuron must have knowledge about the entire network structure [37], which doesn't correspond to the reality: every neuron only has the message of its neighbor neurons.

Another well-known model is navigation model. It suggests that neurons always send information to the neuron that can be reached with the least communication cost [38]. These models achieve the lowest communication cost. Greedy routing in Euclidean space identified paths with 70–100% of optimal signaling efficiency in human, mouse and macaque connectomes [39].

However, the main disadvantage of navigation model is it supposes that neurons know the distance between their neighbors and a desired target region. Recently their still has a lack of evidences that reveal how this knowledge would be given to neurons in brain networks.

Another well-known category of models is the diffusion model. The diffusion model posits that signals propagate through random walk dynamics. This process of propagation does not require individual neurons to possess any prior knowledge beyond their immediate neighboring neurons. Among the most classic of these is the random walk model [40]. In the random walk model, signals are transmitted to randomly selected neighboring nodes with a probability proportional to the connection weights until they reach the target node. For unbiased random walk, the function of random walk model is as follows.

$$P_{ij} = \frac{1}{k_i} \quad (10)$$

Where P_{ij} represent the probability of node i choosing node j . k_i is the degree of node i .

As for biased random walk, for example, if the transition probability depends on the edge weights or certain properties of the nodes, then the transition probability can be adjusted to

$$P_{ij} = \frac{w_{ij}}{\sum_{l \in N(i)} w_{il}} \quad (11)$$

Where w_{ij} is the weight of node i to node j , $N(i)$ is the set of node i .

However, studies have shown that the efficiency of signal transmission through random walks is relatively low [41]. So it can't describe the rapid communication process in the brain.

An effective category is threshold model [42]. The threshold model was originally proposed to characterize collective behavior. In the threshold model, a node's behavior depends on the behavior of its neighboring nodes. Suppose that within a group, nodes can hold one of two states regarding a certain behavior: an active state and a quiescent state. For a node, it will only transition from the quiescent state to the active state if the stimulus given by its neighboring nodes in the active state surpasses a certain threshold; otherwise, it remains in the quiescent state. The condition for node i to adopt the behavior at time $t+1$ can be formulated as follows.

$$a_i(t+1) = 1 \quad \text{if} \quad \frac{1}{k_i} \sum_{j \in N_i} a_j(t) \geq \theta_i \quad (12)$$

Where N_i is the set of neighbors of node i , $a_i(t)$ is the adoption state of node i at time t . θ_i is the threshold of node i . k_i is the degree of node i . The threshold model has been extensively applied in artificial neural networks.

However, how to set the propagation thresholds for different neurons, and how to design the dynamics model between neurons remains a challenge.

3 Data and Methods

3.1 Drosophila Connectome Data Set

We employ the recently released largest Drosophila brain connectome [14], offering a thorough mapping of the entire neural network within a Drosophila female brain. This data set encompasses over 120,000 neurons and 30,000,000 synapses, including detailed information on synaptic connections between neurons. Notably, it provides high-precision 3D coordinates, accurate to the nanometer level, for both cell bodies and synapses. Additionally, this data set offers extensive labeling for various types of neurons. For a more in-depth understanding, please refer to [14] [43] for detailed information.

Table 1 shows the basic properties of the data set. Note that we combine multiple edges between two nodes to calculate network statistic properties. The average degree before combining multiple edges is 501.6 while average degree is 37.01 after combination. It means most of the pairs of neuron has many links.

Apart from that, we draw the curves of degree distribution. From Fig. 1 We found that the distribution of $\log(\text{degree})$ initially appears to be approximately linear, but at the end it exhibits a long-tail distribution, which demonstrate that the original distribution of degree follows a power-law distribution. This result corresponds to the earlier research that neural network also has the power-law property [34].

Table 1: Statistical properties of Drosophila Brain Connectome Graph

Number of Nodes	Number of Edges	Average Degree
131459	32970606	37.01
Average Degree (before combination)	Clustering Coefficient	Eigenvector Centrality
501.6	0.1527	0.0008817

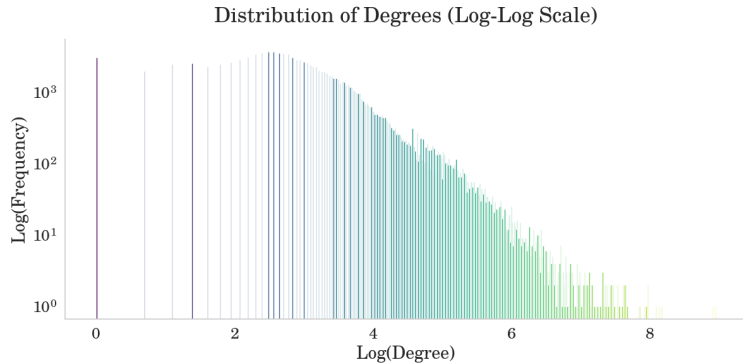


Figure 1: Degree Distribution (Log-Log Scale)

Also, we plot the correlation curves between degree and cell surface area, volume, and cell length (See in Fig. 2). The results indicate the degree distribution is logarithmically linearly correlated with these data. These characteristics of the brain can explain Weber-Fechner’s law [44]: for any sensory pattern, the perceived intensity is a logarithmic function of the physical intensity. The structural changes can only cause a logarithmic change in the average connection strength.

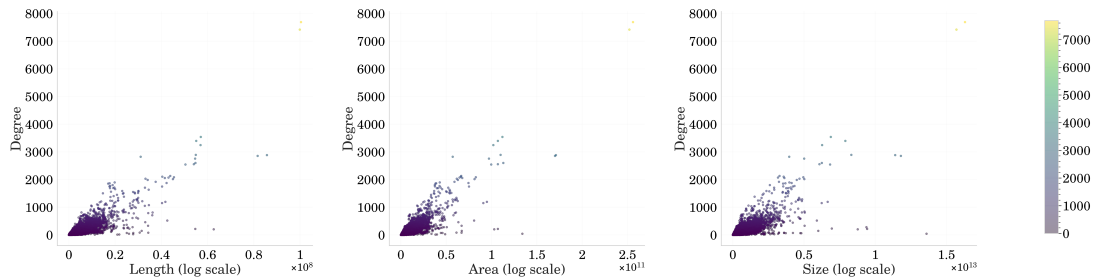


Figure 2: Correlation between degree distribution and neuron characteristics

These statistic results are a valuable supplement to previous findings [45] and are crucial for a deeper understanding of this data set.

3.2 Model

In this section, we introduce the large scale network communication model which consumes less computational resource and can efficiently utilize the network structure. First we introduce the symbol systems in this article.

The original network presentation of neural systems often uses nodes to represent the neurons and using edges to represent the links (chemical synapses, electrical synapses, etc) between neurons [4]. However, this approach has a number of limitations: Firstly, there are more than one link (synapse) between two neurons [46] and the links are spatially and temporally asymmetric. To illustrate, two neurons shown in Fig. 3 have multiple synapses between them, and the dynamical properties of these different synapses may vary. Additionally, due to their spatial locations, the signal transmission delay and the position of action on the downstream neurons are also different, making it difficult to simply merge them.

For this reason, similar to previous research [47], we use the dual method on Drosophila connectome data set. The method is introduced below.

A dual graph is a concept in graph theory which describes a special relationship between graphs. In a dual graph, the nodes and edges of the original graph are interchanged, resulting in a new graph. In simple terms, a dual graph is obtained by replacing the nodes of the original graph with edges, and the edges with nodes. Fig. 4 is an example of an original graph and a dual graph. After being processed, the new graph can be considered

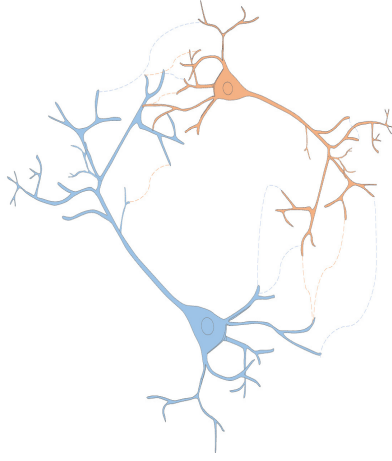
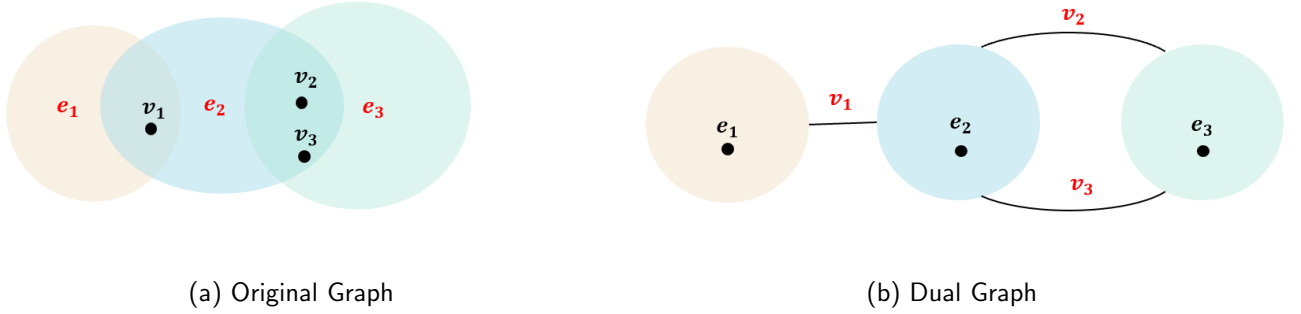


Figure 3: An example of Complex Connection



(a) Original Graph

(b) Dual Graph

Figure 4: An example of original graph and dual graph

to be a hyper graph, whose nodes represent the synapses and links represent the cell body. Then we can use the hyper communication model to describe it.

In order to standardize the symbol system, we use a set to represent the neuronal cell body and use an element to represent a physical link between neurons. We regard the process of messages interactions as the elements' interactions on sets.

Let $N = \{n_1, \dots, n_i, \dots\}$ represent the set of all elements and $E = \{e_1, \dots, e_j, \dots\}$ represent the probable sets of elements. Note that the intersection of sets include some elements, which is formalized as the following manner.

$$e_k \cap e_q = \{n_i | (n_i \in e_k) \wedge (n_i \in e_q)\} \quad (13)$$

Note that union of every element in N and E is the whole graph. Let G represent the graph. The graph's definition is given as follows.

$$G = \bigcup_j e_j = \bigcup_i \{n_i\}. \quad (14)$$

Because neural link is directed, let e_j^+ (e_j^-) represent the set of elements which output (input) the signals, note that $e_j^+ = e_j^+ \cup e_j^-$.

Every neuron and synapse has a activate state (state = 1) or resting state (state = 0). So set the statement of the element i as X_i . $X_i = 1$ if the element n_i is active, otherwise $X_i = 0$. Then let Y_j represent the statement of set e_j . $Y_j = 1$ if the set e_j is active, otherwise $Y_j = 0$.

We use a linear threshold activation function. Then, general transmission function is defined in the following manner,

$$Y_j = \sum_{\{i | e_i^+ \cap e_j^- \neq \emptyset\}} \sum_{n_k \in e_i^+ \cap e_j^-} \sigma(\omega(n_k, e_i, e_j) X_k) \quad (15)$$

where $\omega(n_k, e_i, e_j)$ represents the link weight between set i and set j (specifically, two neurons). Here we consider that the link weight between two neurons is not only related to the neurons themselves, but also to the synapses between them. $\sigma(\cdot)$ is the activate function.

The statement of an neuron will influence the statement of all output synapses. The equation between neuron j and output synapse i is as the following manner.

$$X_i = Y_j \quad (16)$$

The link weights between neurons determine the extent of influence they have on each other. Larger link weights mean a tighter "link" between two neurons. In everyday life, the brain continuously changes the link weights between neurons in response to inputs from the external world, allowing intelligence to emerge from the micro to the macro. Therefore, if researchers want to simulate the process of information propagation in the brain on large scale in a computer, determining the link weights between neurons is essential. However, existing experimental methods are not well-suited for directly measuring the weights between neurons in a whole brain, so adopting some alternative approach is necessary. Below, we introduce two hypotheses that use different methods to estimate the connection weights between neurons.

3.2.1 Average Hypothesis

As previously mentioned, there exists a large number of synapses between two neurons. However, in practical applications, it is difficult to set the parameters for these edges individually. Consequently, a simple assumption naturally arises: assuming that the source neuron has the same influence on the target neuron through every synapse. We propose an assumption that every synapse is equivalent, which is widely used in neuron graph statistics analysis [45]. That is to say,

$$\omega(n_k, e_i, e_j) = 1 \quad (17)$$

Then the normalized equation is as follows.

$$Y_j = \sigma\left(\frac{\sum_{\{i|e_i^+ \cap e_j^- \neq \emptyset\}} \sum_{n_k \in e_i^+ \cap e_j^-} \sigma(\omega(n_k, e_i, e_j)X_k)}{\text{Max}(\{\omega(n_k, e_i, e_j)|e_i^+ \cap e_j^- \neq \emptyset, n_k \in e_i^+ \cap e_j^-\})}\right) \quad (18)$$

3.2.2 Distance Hypothesis

The continuous evolution of organisms has led to the brain's spatial structure being highly complex, with a small area possibly containing a large number of neurons. Besides, a fact is messages are transmitted through bioelectric currents. Assuming that the distance is longer, the resistance will be greater, resulting in a smaller communication effect. Based on this, there emerges a hypothesis: Is the strength of interactions between neurons inversely proportional to the spatial distance between them? So in the distance hypothesis we assume that the impact of input synapses on neurons is inversely proportional to the distance between them. Then the norm can be formulated as follows.

$$\omega(n_k, e_i, e_j) = (\|\vec{r}_k\|^2 - \|\vec{r}_j\|^2)^{\frac{1}{2}} \quad (19)$$

Where r_k, r_j are the center position vector of synapse and cell body, respectively.

Then the transmission function is defined as the following manner.

$$Y_j = \sigma\left(\frac{\sum_{\{i|e_i^+ \cap e_j^- \neq \emptyset\}} \sum_{n_k \in e_i^+ \cap e_j^-} \sigma(\omega(n_k, e_i, e_j)X_k)}{\text{Max}(\{\omega(n_k, e_i, e_j)|e_i^+ \cap e_j^- \neq \emptyset, n_k \in e_i^+ \cap e_j^-\})}\right) \quad (20)$$

3.3 Evaluation Criteria

In previous study, researchers used classic indicators such as signaling cost and activation time to evaluate the quality of the model [11] [48] [49]. However, these indicators can't prove the model accords with the true communication process even if the activation time is short and the signaling cost is minimum, etc. To better assess whether a model can reflect the real situation of brain communication, we use the percentage of activated neurons in regions that should work under a certain stimulus. To illustrate, if the brain gets a visual stimulus, the region related to vision should work while the region not related to vision should keep in a resting state. Then we record the percentage of neurons activated and if regions related to the certain function have a significant higher activation percentage than the average activation percentage of the whole brain, we call it a quasi-real activation pattern.

We define the consistency indicator C . The consistency indicator C in region r which has a certain function (visual, olfactory, etc) is defined in the following manner.

$$C_r = N_r^{act} / N_r \quad (21)$$

Where N_r^{act} represents the number of neurons activated in area r at the final state, N_r represent the number of neurons in area r and N represent the total number of neurons.

3.4 Large Spatial Network Visualization

The visualization software of experiment observation on large spatial networks is important for researchers [50] [51]. However, there is still a lack of visualization system that can observe information propagation on large spatial networks in real-time, which poses difficulties in experiment. To observe directly the communication progress on this super large *Drosophila* connectome, we develop a large spatial network visualization software.

The drawing part mainly employs the Canvas provided by HTML5 and we use the Three.js based on WebGL technology to achieve spatial network visualization effects, while the user interface display is constructed by Vue.js, providing users with an intuitive and interactive interface to display and analyze data. Fig. 5 is an example of the 3D visualization system. This software will be made available to other researchers with the author's permission.

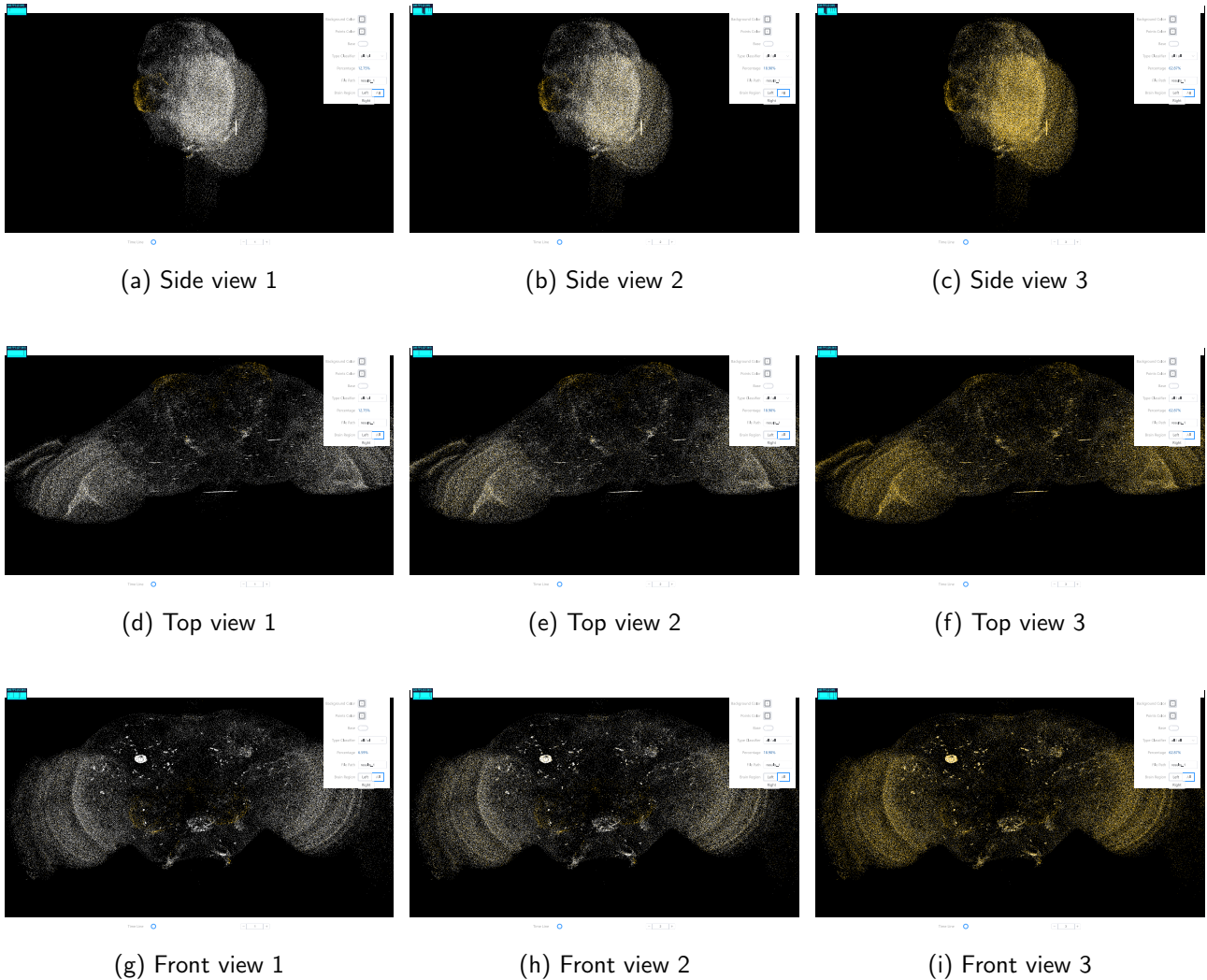


Figure 5: Visualization of Spatial *Drosophila* Brain Network

3.4.1 Front End Technical Details

We use the Vue.js framework to build the user interface. Vue.js is a popular JavaScript framework that simplifies the development of web applications through componentization, enabling the creation of front-end interfaces with rich interactivity and good user experience.

The rendering of three-dimensional complex networks relies heavily on the Three.js library. Three.js is a powerful JavaScript library for creating and displaying 3D graphics. It offers a rich set of 3D objects, materials, lights, and animations, allowing for the easy creation of high-quality 3D scenes and objects.

To improve rendering performance, GPU acceleration technology is utilized. GPU acceleration takes advantage of the computational power of the Graphics Processing, significantly enhancing rendering speed and efficiency through parallel processing and stream processing modes. The GPU acceleration capabilities of

Three.js, especially through the creation of point objects using `Float32BufferAttribute`, which contains their position information in three-dimensional space, greatly enhance the rendering speed and smoothness.

3.4.2 Back End Technical Details

We use the Spring Boot framework, an open-source framework based on Java for quickly building independent, production-grade Spring applications. With Spring Boot, backend services can be rapidly set up to provide RESTful API interfaces for frontend consumption. The backend also utilizes the PostgreSQL database to store network data.

Besides, We use PostgreSQL, which is a powerful open-source relational database management system that offers a rich set of data types and robust querying capabilities. To store 3D network data, we leverage PostgreSQL's JSONB type, which allows storing JSON-formatted data within PostgreSQL and provides a series of functions and operators for querying and manipulating this data. With the JSONB type, information about nodes and edges in the network can be stored, enabling fast querying and updating operations.

4 Experimental Results and Analysis

In this part we introduce the experimental results and analysis. Above all, we introduce the activation pattern experiment. We give different stimuli and record the activation pattern of different neurons. In addition, we give a unilateral stimulus (stimulus one hemisphere) and record the bilateral response of neurons. Finally, to prove the network structure matters in brain network communication, we calculate the average physical and network distance between different areas.

4.1 Experimental Settings

The basic methodology of the experiment is described as follows. In this study, a continuous stimulus signal (binary 0-1 signal) is applied to a subset of input neurons (such as visual or olfactory neurons) in the brain. Subsequently, we compute the signal's propagation process within the brain and record the responses of both intermediate and output neurons. The evaluation criterion is determined by calculating the ratio of neurons that ought to be activated to those that are actually activated in a specific area. Given that the brain functions as a type of shallow neural network [52], we document the outcomes at an iteration step size of 5, by which point the majority of neurons have achieved a state of stability. Moreover, as the input remains constant and no randomization parameters have been introduced, the outcomes of each experiment are consistent, eliminating the need for repetition.

Next, we will introduce the background knowledge of the neurons involved in this paper. Here are introductions of these neurons.

Optic neurons, also known as retinal ganglion cells, are the first neurons in the visual pathway. They receive signals from the photoreceptor cells in the retina and transmit this information via the optic nerve to the brain. These neurons play a crucial role in carrying visual stimuli from the eye to the brain, where further processing and interpretation of the visual information occur.

Visual projection neurons are a type of neuron found in the visual system that transmit visual information from one region of the brain to another. They play a crucial role in processing and relaying visual signals from the retina to various visual centers in the brain, including the thalamus, hypothalamus, and primary visual cortex (V1), among others.

Antennal Lobe Input Neurons (ALINs) are primarily olfactory sensory neurons (OSNs) that carry olfactory information from the sensory structures, such as the antennae and maxillary palps, directly to the antennal lobe. Each OSN expresses a specific odorant receptor and responds to particular chemical cues. The axons of these neurons synapse with projection neurons and local neurons within the glomeruli of the antennal lobe.

Antennal Lobe Projection Neurons (ALPNs) transmit the olfactory information in the antennal lobe. These neurons receive input from the olfactory sensory neurons within the glomeruli and project their axons to other brain areas, such as the mushroom body and the lateral horn, where further processing and integration of olfactory information occur.

Antennal Lobe Output Neurons (ALONs) refer to the projection neurons that serve as the primary output pathways of the antennal lobe, sending processed olfactory information to higher brain regions.

Antennal Lobe Local Neurons (ALLNs) are inter neurons that are confined to the antennal lobe. They typically have processes (dendrites and axons) that branch extensively within the antennal lobe and form connections with multiple glomeruli. These neurons play a critical role in modulating and refining the olfactory information by providing inhibitory or excitatory input to projection neurons and other local neurons, thus shaping the olfactory responses and contributing to odor discrimination and perception.

For further information, please read [43].

4.2 Activation Patterns on Different Type of Neurons

Primarily, to validate the efficacy of our model in modifying signal transmission between input and output neurons, we showcase the activation patterns of intermediate and output neurons throughout the information transmission process. This demonstration serves to substantiate that our model accurately reflects real-world scenarios, shaping a quasi-real activation pattern.

The specific idea for the experiment is following : we stimulate different types of neurons (such as visual input neurons, olfactory neurons, etc.), and record the rate that neurons that are activated in different brain areas. If a specific stimulus causes a significantly greater response than the average in the brain area that it is theoretically supposed to activate, then it is considered that the model can generate a quasi-real activation pattern in the brain. We give 2 types of input neurons (visual, olfactory) stimulus display 6 type of neurons: optic (visual), visual_projection (visual), ALLN (olfactory), ALIN (olfactory), ALPN (olfactory) and ALON (olfactory).

To demonstrate the importance of network structure, we add a comparative model that randomly reconnects networks. Specifically, we calculate the average network distance from input neurons (visual/olfactory) to corresponding neurons (optic, visual_projection/ALLN, ALPN, ALON, ALLN), round it to the nearest integer to determine the average layer of that neuron, and then randomly swap the connections between nodes within each layer.

Fig. 6 shows the activation patterns of different models. The different neuron types are on the horizontal ordinate and the activation percentage is on the vertical ordinate. The horizontal line represents the percentage of activated neurons in the whole brain. From Fig. 6 we can find that under the average hypothesis, visual stimulus cause a strong impact (significantly more than average) on visual neurons (optic, visual projection) while causing a slight impact (significantly less than average) on other type of neurons. Specifically, under visual stimulus, in response to visual stimuli, the optic (vision related area) exhibit a 10.26% higher activation rate compared to the average level, while no olfactory-related neurons are activated. In addition, olfactory stimulus cause a strong impact (significantly bigger than average level) on olfactory neurons (ALLN, ALIN, ALPN, ALON), exceeding the average level by 81.49%. And it cause a slight impact (significantly less than average) on other type of neurons. For example, it only activates 0.04% of optic and 0.79% of visual_projection.

Furthermore, the results are not as significant on the distance model. Some incorrect areas were activated: The activate rate of ALLN is only 7.08%, with a 5.16% difference from the average level (Fig. 6(c)). Besides, ALIN, ALPN and ALLN, which should not be activated, have activate rates of 12.50%, 0.15%, and 1.89%, respectively (Fig. 6(c)). These results indicate that whether distance hypothesis can describe the actual situation remains to be discussed, which is a refutation for previous research [53].

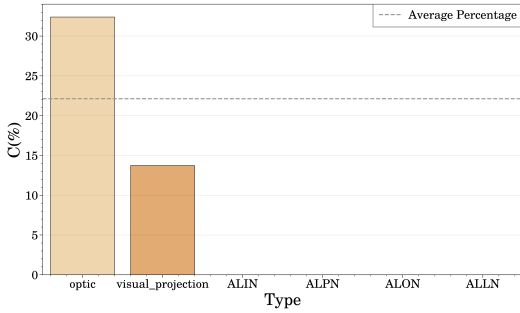
As for the shuffle model, the ALIN, ALPN, ALON and ALLN which should not be activated have activate rates of 70.00%, 54.13%, 61.25% and 62.31%, respectively (Fig. 6(e)). Although these activate rates do not meet the average level, they are significant activation rates that means many neruons are activated incorrectly. Moreover, optic and visual_projection are activated incorrectly, with activate rates of 55.11% and 42.52%, respectively (Fig. 6(f)). Besides, ALLN, ALPN, ALON, and ALLN which are supposed to exceed the average level are actually lower than the average level by 0.01%, 17.74%, 21.25% and 9.34%, respectively (Fig. 6(f)).

These results indicate that after shuffling the network structure, the original quasi-real activation patterns completely disappear. It means the real network structure matters in generating the quasi-real activation patterns. In addition, even just designing simple models, it is feasible to simulate the propagation of information in the brain at the level of neurons and generate a quasi-real activation pattern.

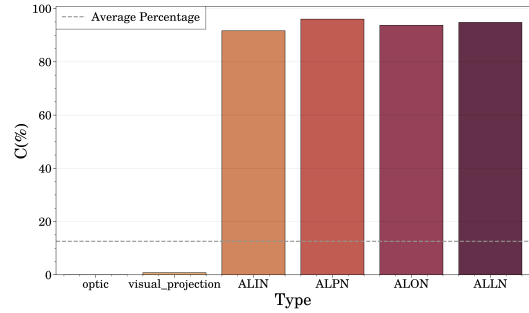
4.3 Distances between Input and Activation Areas

In the previous section, the quasi-real activation patterns on different type of neurons of the brain was presented. Through observation, this relationship was identified, and a quasi-real activation pattern was observed in the drosophila brain. There is an issue here: Is the quasi-real activation pattern determined by the brain network's structure, the spatial structure of the brain, or the quality of the network communication model? Based on the puzzle, we calculated the average network distance and spatial distance between different areas of the brain network. The optic and visual_projection area are related to vision and ALLN, ALIN, ALON, ALPN, LHCENT and LHLN are related to olfactory. The results are presented in Tab. 2.

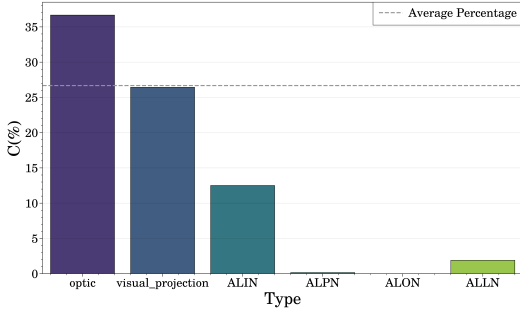
From Tab. 2, it is evident that neurons which are closer in spatial distance are not necessarily easier to activate. For example, all areas and visual input neurons have similar average spatial distances, but the quasi-real activation patterns can only be observed in specific neural types (optic, visual_projection). In contrast, the average network distance between input neurons and neurons should be activated is closer than irrelevant neurons. For instance, the distance between visual input neurons and optic, visual_projection are 5.7018 and 5.7432, respectively. And the distance between visual input neurons and ALLN, ALIN, ALON, ALPN, LHCENT, LHLN which are irrelevant with vision are 6.6442, 6.2350, 6.1506, 6.5380, 6.3094 and 6.8206, respectively. The network distance of neurons related to visual input neurons is generally closer than the distances of unrelated



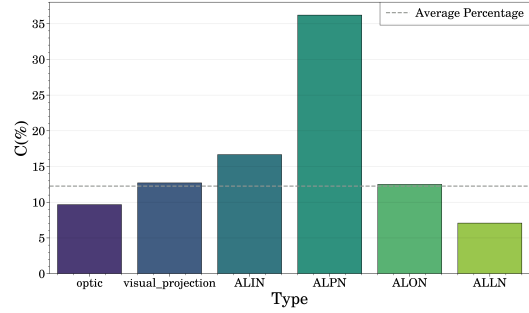
(a) visual stimulus, average model



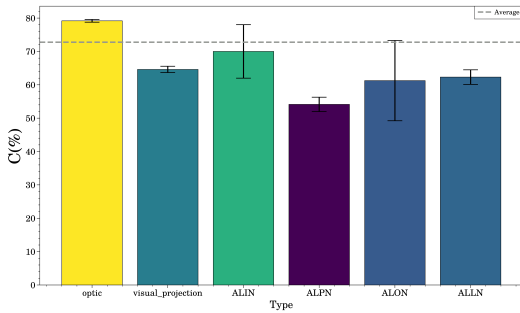
(b) olfactory stimulus, average model



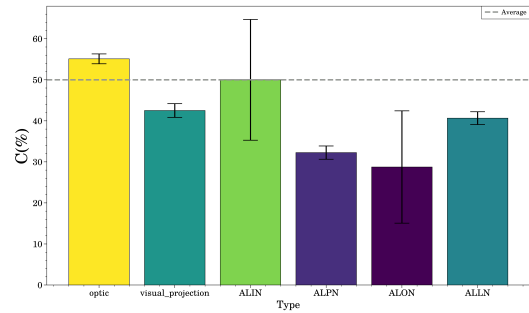
(c) visual stimulus, distance model



(d) olfactory stimulus, distance model



(e) visual stimulus, shuffle model



(f) olfactory stimulus, shuffle model

Figure 6: Experiment of intrinsic neurons' activation. $\sigma_0 = 0.8$. For shuffle model, we conduct 5 repeated experiments and take the average and standard deviation.

neurons. Besides, The average network distance of neurons related to olfactory input neurons is approximately twice as close as the distance of unrelated neurons. These results indicates that compared to spatial distance, the average network distance between input neurons and their corresponding activation areas is closer, meaning that compared to spatial structure, network structure is more important, determining these quasi-real activation patterns of the brain network.

This results reflect the importance of network structure in neural networks, that is, the ability to reproduce certain functions of the brain by considering only the network structure.

4.4 Bilateral Response under Unilateral Stimulus

In real life, the left and right hemispheres cooperate to perform complex tasks. We are interested in whether network models can simulate this cooperative effect to some extent. So we administer a unilateral stimulus to the input neurons and monitor the varying activation ratios across both hemispheres. More precisely, we independently simulate visual input neurons in the left and right hemispheres and record the rate of activated neurons in each hemisphere over time. Figure 7 illustrates the curve depicting how the response ratio evolves with each time step. It's noteworthy that when simulating one hemisphere alone, visual processing neurons in both hemispheres are activated. At time step 5, the unstimulated hemisphere begins to have a activate pattern, which corresponds to the hypothesis of shallow connection [52]. Furthermore, our observations reveal a concurrent effect: the activation pattern in one hemisphere mirrors that in the unstimulated hemisphere.

These findings are reflective of reality. Although the left and right hemispheres of the brain possess certain functional specializations, they also demonstrate a synergistic effect. Typically, they collaborate to fulfill specific

Table 2: Spatial and network distance between input and main areas. The unit of spatial distance is nm and the unit of network distance is the number of edges in the shortest path.

distance type	Area Name	optic	visual_projection	ALLN	ALIN
	Neuron type				
Spatial Distance	Visual Input Neurons	365012	354725	351919	348901
	Olfactory Input Neurons	302690	251144	110827	173345
		ALON	ALPN	LHCENT	LHLN
	Visual Input Neurons	346925	348517	362825	366013
	Olfactory Input Neurons	123179	115089	212515	246719
Network Distance		optic	visual_projection	ALLN	ALIN
	Visual Input Neurons	5.7018	5.7432	6.6442	6.2350
	Olfactory Input Neurons	5.7967	5.1706	3.4458	3.3845
		ALON	ALPN	LHCENT	LHLN
	Visual Input Neurons	6.1506	6.5380	6.3094	6.8206
	Olfactory Input Neurons	3.6312	3.6820	3.9557	3.9758

functions [54]. For instance, during complex cognitive tasks, both hemispheres coordinate their efforts to contribute to task completion. Even when simulating input to neurons on just one side of the brain, our model reveals similar synergistic effects, indirectly attesting to the model’s effectiveness. Besides, the mirror effect align with real situation, underscoring the brain’s resilience as a system. In instances of disease or physical damage leading to impairment in one hemisphere, this interconnected structure supports the continuation of critical functions, such as vision. Visually, the shape of the brain appears to be physically similar, but whether the

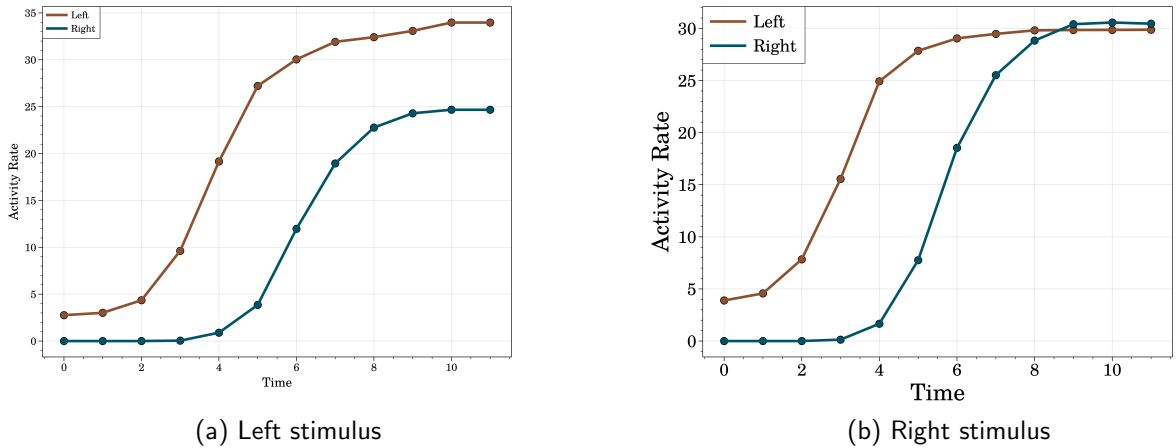


Figure 7: Experiment of activation rate under single stimulus. We set threshold $\sigma_0 = 0.8$.

network structures are similar remains unknown. To explore the principle behind similar responses caused by a unilateral stimulus, we calculated the degree, clustering coefficient, and eigenvector centrality distribution for each hemisphere. The Pearson correlation coefficient of degree, clustering coefficient, and eigenvector centrality vector is 0.9986, 0.9988, and 0.9991, respectively. According to Fig. 8, these statistical indicators for both hemispheres are extremely similar, indicating that the brain exhibits strong symmetry in network structure.

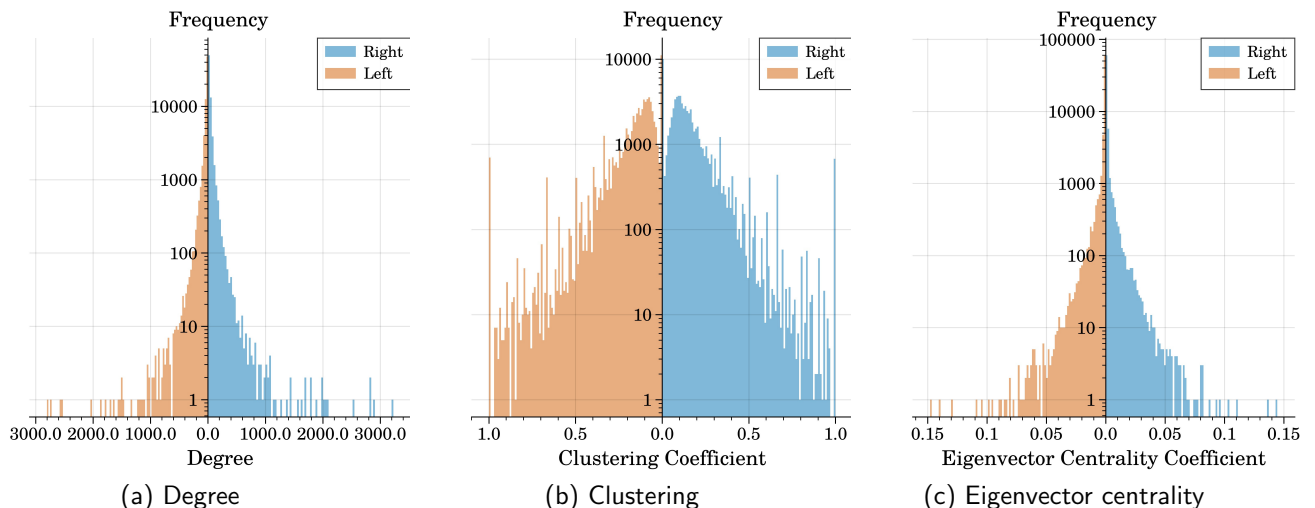


Figure 8: Degree, clustering coefficient, and eigenvector centrality distribution

5 Conclusion

Considering the insufficient evidence supporting the vitalness of network structure in brain message transmission and the effectiveness of network models in simulating brain activation patterns, we propose a large scale network communication model based on simple propagation rules. We also design an evaluation criteria to compare real and simulated activation patterns. Our research utilizes the largest adult *Drosophila* connectome data set, where we analyze the basic statistical properties and explore the relationship between neuron length, area, size, and connectivity degree. Experimental results demonstrate that our model produces an activation pattern across the brain that closely resembles reality when subjected to identical stimulus on input neurons. This result strongly suggests that even with simple propagation rules, network models can approximate the brain’s activation patterns. Besides, when changing the network structure, there is an incorrect activation pattern on the brain network. It is an evidence that network structure matters in generation real brain activation patterns. Furthermore, to prove network structure matters rather than propagation rules or spatial structure, we assess the network and spatial distances across different areas, discovering that the average network distance between input neurons and their corresponding activation areas is shorter. Notably, applying unilateral stimulus to input neurons elicit bilateral responses, mirroring bilateral brain coordination in reality and providing additional evidence that simple network models can closely replicate reality. Moreover, we calculate the statistic properties and find that the network structures of two hemispheres are extremely similar. We also make a large spatial network visualization software. This research reveals network models can reach the brain’s quasi-activation pattern even with simple propagation rules. Besides, it provides evidence that network structure matters in brain activity pattern generation. Other artificial neural network research may need to make their own structure close to the real network structure. However, it does not perfect the model to achieve a full-activation pattern. Future research could enable complete simulation of brain behavior by optimizing propagation rules and automatically adjusting link weights, paving the way for achieving genuine artificial intelligence.

6 Acknowledgement

This work was supported by the National Natural Science Foundation of China (72025405, 72088101), the National Social Science Foundation of China (22ZDA102), the Hunan Science and Technology Plan Project (2020TP1013, 2020JJ4673, 2023JJ40685), the Innovation Team Project of Colleges in Guangdong Province (2020KCXTD040), and the Postgraduate Scientific Research Innovation Project of Hunan Province (XJCX2023095). The authors declare that they have no conflict of interest.

References

- [1] Irwin B Levitan and Leonard K Kaczmarek. *The neuron: cell and molecular biology*. Oxford University Press, USA, 2015.
- [2] Talia N Lerner, Li Ye, and Karl Deisseroth. Communication in neural circuits: tools, opportunities, and challenges. *Cell*, 164(6):1136–1150, 2016.

- [3] Anthony Zador, Sean Escola, Blake Richards, Bence Ölveczky, Yoshua Bengio, Kwabena Boahen, Matthew Botvinick, Dmitri Chklovskii, Anne Churchland, Claudia Clopath, et al. Catalyzing next-generation artificial intelligence through neuroai. *Nature communications*, 14(1):1597, 2023.
- [4] Andrea Avena-Koenigsberger, Bratislav Misic, and Olaf Sporns. Communication dynamics in complex brain networks. *Nature Reviews Neuroscience*, 19(1):17–33, 2018.
- [5] Lin Zhao, Lu Zhang, Zihao Wu, Yuzhong Chen, Haixing Dai, Xiaowei Yu, Zhengliang Liu, Tuo Zhang, Xintao Hu, Xi Jiang, et al. When brain-inspired ai meets agi. *Meta-Radiology*, page 100005, 2023.
- [6] Dániel L Barabási, Ginestra Bianconi, Ed Bullmore, Mark Burgess, SueYeon Chung, Tina Eliassi-Rad, Dileep George, István A Kovács, Hernán Makse, Thomas E Nichols, et al. Neuroscience needs network science. *Journal of Neuroscience*, 43(34):5989–5995, 2023.
- [7] Cornelis J Stam. Modern network science of neurological disorders. *Nature Reviews Neuroscience*, 15(10):683–695, 2014.
- [8] Danielle S Bassett and Olaf Sporns. Network neuroscience. *Nature Neuroscience*, 20(3):353–364, 2017.
- [9] Ernesto Estrada and Naomichi Hatano. Communicability in complex networks. *Physical Review E*, 77(3):036111, 2008.
- [10] Martin Rosvall, Andreas Grönlund, Petter Minnhagen, and Kim Sneppen. Searchability of networks. *Physical Review E*, 72(4):046117, 2005.
- [11] Caio Seguin, Olaf Sporns, and Andrew Zalesky. Brain network communication: concepts, models and applications. *Nature Reviews Neuroscience*, 24(9):557–574, 2023.
- [12] Douglas S Portman. Neural networks mapped in both sexes of the worm, 2019.
- [13] Michael Winding, Benjamin D Pedigo, Christopher L Barnes, Heather G Patsolic, Youngser Park, Tom Kazimiers, Akira Fushiki, Ingrid V Andrade, Avinash Khandelwal, Javier Valdes-Aleman, et al. The connectome of an insect brain. *Science*, 379(6636):eadd9330, 2023.
- [14] Sven Dorckenwald, Arie Matsliah, Amy R Sterling, Philipp Schlegel, Szi-Chieh Yu, Claire E McKellar, Albert Lin, Marta Costa, Katharina Eichler, Yijie Yin, et al. Neuronal wiring diagram of an adult brain. *bioRxiv*.
- [15] Alan L Hodgkin and Andrew F Huxley. A quantitative description of membrane current and its application to conduction and excitation in nerve. *The Journal of physiology*, 117(4):500, 1952.
- [16] Henry Clavering Tuckwell. *Introduction to theoretical neurobiology: linear cable theory and dendritic structure*, volume 1. Cambridge University Press, 1988.
- [17] Suhas Kumar, Xinxin Wang, John Paul Strachan, Yuchao Yang, and Wei D Lu. Dynamical memristors for higher-complexity neuromorphic computing. *Nature Reviews Materials*, 7(7):575–591, 2022.
- [18] Allan R Willms, Deborah J Baro, Ronald M Harris-Warrick, and John Guckenheimer. An improved parameter estimation method for hodgkin-huxley models. *Journal of computational neuroscience*, 6:145–168, 1999.
- [19] Samanwoy Ghosh-Dastidar and Hojjat Adeli. Spiking neural networks. *International journal of Neural Systems*, 19(04):295–308, 2009.
- [20] Petr Lansky and Susanne Ditlevsen. A review of the methods for signal estimation in stochastic diffusion leaky integrate-and-fire neuronal models. *Biological Cybernetics*, 99(4):253–262, 2008.
- [21] Quoc Trung Pham, Thu Quyen Nguyen, Phuong Chi Hoang, Quang Hieu Dang, Duc Minh Nguyen, and Huy Hoang Nguyen. A review of snn implementation on fpga. In *2021 international conference on multimedia analysis and pattern recognition (MAPR)*, pages 1–6. IEEE, 2021.
- [22] Ali Lotfi Rezaabad and Sriram Vishwanath. Long short-term memory spiking networks and their applications. In *International Conference on Neuromorphic Systems 2020*, pages 1–9, 2020.
- [23] Siti Aisyah Mohamed, Muhaini Othman, and M Hafizul Affi. A review on data clustering using spiking neural network (snn) models. *Indonesian Journal of Electrical Engineering and Computer Science*, 15(3):1392–1400, 2019.

- [24] Gege Zhan, Zuoting Song, Tao Fang, Yuan Zhang, Song Le, Xueze Zhang, Shouyan Wang, Yifang Lin, Jie Jia, Lihua Zhang, et al. Applications of spiking neural network in brain computer interface. In *2021 9th International Winter Conference on Brain-Computer Interface (BCI)*, pages 1–6. IEEE, 2021.
- [25] Eugene M Izhikevich and Gerald M Edelman. Large-scale model of mammalian thalamocortical systems. *Proceedings of the National Academy of Sciences*, 105(9):3593–3598, 2008.
- [26] Chris Eliasmith, Terrence C Stewart, Xuan Choo, Trevor Bekolay, Travis DeWolf, Yichuan Tang, and Daniel Rasmussen. A large-scale model of the functioning brain. *Science*, 338(6111):1202–1205, 2012.
- [27] Yi Zeng, Dongcheng Zhao, Feifei Zhao, Guobin Shen, Yiting Dong, Enmeng Lu, Qian Zhang, Yinqian Sun, Qian Liang, Yuxuan Zhao, et al. Braincog: A spiking neural network based, brain-inspired cognitive intelligence engine for brain-inspired ai and brain simulation. *Patterns*, 4(8), 2023.
- [28] Peter A Robinson, Christopher J Rennie, and James J Wright. Propagation and stability of waves of electrical activity in the cerebral cortex. *Physical Review E*, 56(1):826, 1997.
- [29] Michael Breakspear, James A Roberts, John R Terry, Serafim Rodrigues, Neil Mahant, and Peter A Robinson. A unifying explanation of primary generalized seizures through nonlinear brain modeling and bifurcation analysis. *Cerebral Cortex*, 16(9):1296–1313, 2006.
- [30] Ed Bullmore and Olaf Sporns. The economy of brain network organization. *Nature Reviews Neuroscience*, 13(5):336–349, 2012.
- [31] Christopher W Lynn and Danielle S Bassett. The physics of brain network structure, function and control. *Nature Reviews Physics*, 1(5):318–332, 2019.
- [32] Alex Fornito, Andrew Zalesky, and Edward Bullmore. *Fundamentals of brain network analysis*. Academic press, 2016.
- [33] Bin Zhou, Xin Lu, and Petter Holme. Universal evolution patterns of degree assortativity in social networks. *Social Networks*, 63:47–55, 2020.
- [34] Dante R Chialvo. Critical brain networks. *Physica A: Statistical Mechanics and its Applications*, 340(4):756–765, 2004.
- [35] Eyal Gal, Michael London, Amir Globerson, Srikanth Ramaswamy, Michael W Reimann, Eilif Muller, Henry Markram, and Idan Segev. Rich cell-type-specific network topology in neocortical microcircuitry. *Nature Neuroscience*, 20(7):1004–1013, 2017.
- [36] Stefano Pallottino and Maria Grazia Scutella. Shortest path algorithms in transportation models: classical and innovative aspects. In *Equilibrium and advanced transportation modelling*, pages 245–281. Springer, 1998.
- [37] Marian Boguna, Dmitri Krioukov, and Kimberly C Claffy. Navigability of complex networks. *Nature Physics*, 5(1):74–80, 2009.
- [38] M Ángeles Serrano, Dmitri Krioukov, and Marián Boguná. Self-similarity of complex networks and hidden metric spaces. *Physical Review Letters*, 100(7):078701, 2008.
- [39] Caio Seguin, Martijn P Van Den Heuvel, and Andrew Zalesky. Navigation of brain networks. *Proceedings of the National Academy of Sciences*, 115(24):6297–6302, 2018.
- [40] Edward A Codling, Michael J Plank, and Simon Benhamou. Random walk models in biology. *Journal of the Royal society interface*, 5(25):813–834, 2008.
- [41] Andrea Avena-Koenigsberger, Joaquín Goñi, Richard F Betzel, Martijn P van den Heuvel, Alessandra Griffa, Patric Hagmann, Jean-Philippe Thiran, and Olaf Sporns. Using pareto optimality to explore the topology and dynamics of the human connectome. *Philosophical Transactions of the Royal Society B: Biological Sciences*, 369(1653):20130530, 2014.
- [42] Mark Granovetter. Threshold models of collective behavior. *American journal of sociology*, 83(6):1420–1443, 1978.
- [43] Philipp Schlegel, Yijie Yin, Alexander S Bates, Sven Dorkenwald, Katharina Eichler, Paul Brooks, Daniel S Han, Marina Gkantia, Marcia Dos Santos, Eva J Munnelly, et al. A consensus cell type atlas from multiple connectomes reveals principles of circuit stereotypy and variation. *Biorxiv: the Preprint Server for Biology*, 2023.

- [44] Kazukayasu Shigemoto. Weber-fechner’s law and demand function. *arXiv preprint physics/0303118*, 2003.
- [45] Albert Lin, Runzhe Yang, Sven Dorckenwald, Arie Matsliah, Amy R Sterling, Philipp Schlegel, Szi-chieh Yu, Claire E McKellar, Marta Costa, Katharina Eichler, et al. Network statistics of the whole-brain connectome of drosophila. *bioRxiv*, 2023.
- [46] Michael Fauth, Florentin Wörgötter, and Christian Tetzlaff. The formation of multi-synaptic connections by the interaction of synaptic and structural plasticity and their functional consequences. *PLoS Computational Biology*, 11(1):e1004031, 2015.
- [47] Márton Pósfai, Balázs Szegedy, Iva Bačić, Luka Blagojević, Miklós Abért, János Kertész, László Lovász, and Albert-László Barabási. Impact of physicality on network structure. *Nature Physics*, pages 1–8, 2023.
- [48] Marcus Kaiser, Matthias Goerner, and Claus C Hilgetag. Criticality of spreading dynamics in hierarchical cluster networks without inhibition. *New Journal of Physics*, 9(5):110, 2007.
- [49] Caio Seguin, Maciej Jedynek, Olivier David, Sina Mansour, Olaf Sporns, and Andrew Zalesky. Communication dynamics in the human connectome shape the cortex-wide propagation of direct electrical stimulation. *Neuron*, 111(9):1391–1401, 2023.
- [50] Lothar Krempel. Network visualization. *The SAGE handbook of social network analysis*, pages 558–577, 2011.
- [51] James Moody, Daniel McFarland, and Skye Bender-deMoll. Dynamic network visualization. *American Journal of Sociology*, 110(4):1206–1241, 2005.
- [52] Mototaka Suzuki, Cyriel MA Pennartz, and Jaan Aru. How deep is the brain? the shallow brain hypothesis. *Nature Reviews Neuroscience*, 24(12):778–791, 2023.
- [53] James C Pang, Kevin M Aquino, Marianne Oldehinkel, Peter A Robinson, Ben D Fulcher, Michael Breakspear, and Alex Fornito. Geometric constraints on human brain function. *Nature*, 618(7965):566–574, 2023.
- [54] Larry W Swanson. *Brain architecture: understanding the basic plan*. Oxford University Press, USA, 2012.